Inorganic Chemistry

Article

pubs.acs.org/IC

Linear or Cyclic Clusters of Cu(II) with a Hierarchical Relationship

Gavin A. Craig,[†] Mike Schütze,[†] David Aguilà,[†] Olivier Roubeau,[‡] Jordi Ribas-Ariño,[§] Sergi Vela,[§] Simon J. Teat,[∥] and Guillem Aromí*[,†]

[†]Departament de Química Inorgànica, Universitat de Barcelona, Diagonal 645, 08028 Barcelona, Spain

[‡]Instituto de Ciencia de Materiales de Aragón (ICMA), CSIC and Universidad de Zaragoza, Plaza San Francisco s/n, 50009 Zaragoza, Spain

[§]Departament de Química Física and IQTCUB, Universitat de Barcelona, Diagonal 645, 08028 Barcelona, Spain

[∥]Advanced Light Source, Berkeley Laboratory, 1 Cyclotron Road, Berkeley, California 94720, United States

Supporting Information

ABSTRACT: The polydentate ligand 2,6-bis(5-(2-hydroxyphenyl)-pyrazol-3-yl)-pyridine, H_4L, exhibits a series of coordination pockets favoring the establishment of metal sequences with predetermined motifs, together with a degree of flexibility for the formation of clusters with various overall topologies. With Cu(II) under strong basic conditions it has a marked tendency to stabilize a cyclic $[Cu_{16}L_8]$ cluster. The sequential formation of this compound via $[Cu_7L_8]^{2-}$ intermediates, recognized in its structure, is suggested by crystallographic evidence, which shows the persistent formation of the complex salt $(NBu_4)_2[Cu_7L_8]$ in the presence of the organic cation. Also, the crystallographic identification of the related cluster $[Cu_{11}L_5(OH)_2(py)_{12}]$ from similar reaction conditions underscores the rich multiplicity of species attainable from this simple reaction system.

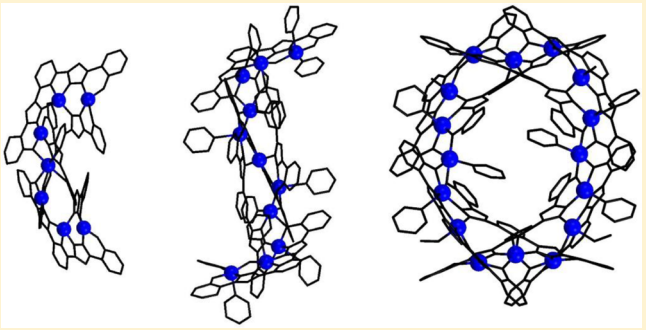

INTRODUCTION

The vast and fascinating topic of cluster coordination chemistry has relied initially on the synthetic approach termed serendipitous self-assembly. By this method, small bridging ligands and metal ions are allowed to react and stabilize as a preferred multinuclear aggregate among the countless possibilities offered by a large number of degrees of freedom.[1−3] In general, the precise structure of the resulting cluster cannot be anticipated, and only after a first compound has been identified is it possible to build up on a given system and reach some level of control.[3−6] Despite this lack of predictability, the method has furnished the seeds from which highly relevant areas in molecular materials science have bloomed, such as the discovery[7] and development of single molecule magnets[8,9] and molecular magnetic refrigerants,[10,11] or recent proposals for using the spin of clusters in quantum computing.[12,13] A parallel methodology for the preparation of higher nuclearity complexes has been the design of multidentate ligands that, because of structural constraints or rigidity, offer a limited number of degrees of freedom for coordinating to metals.[14] The topologies of such ligands, together with the geometrical requirements of the metals with which they are made to react, allow the precise prediction of the final structure. Distinguished families of compounds resulting from this approach have been the group of metallohelicates,[15] the series of molecular grids,[16] or the category of molecular metal wires.[17,18] There is however a large number of polynuclear aggregates, the preparation of which cannot be categorized under either of these two types, but rather somewhere in between. These are normally made with polydentate ligands that impose some structural constraints but offer enough versatility so that only certain aspects of the final structure may be anticipated but not the whole ensemble. In this context, the synergy of serendipity and rational design in coordination chemistry has been highlighted in the literature.[19] The lability of the bonds involved in this chemistry suggests the possibility of *error corrections* in the process of formation of the most stable product (the one *favored* by thermodynamics). A recent paper reports the mapping of the self-assembly process of a heterometallic grid cluster of a bis-pyrazolyl-tris-pyridyl ligand.[20] Thus, the transit through intermediate clusters, and also some subproducts considered as correctable errors, could be monitored by time-resolved ESI-MS techniques. Along these lines, the formation of $[Cd_{16}]$ and $[Cu_{12}]$ homoleptic cages made with a related naphthalenyl-spaced bis(pyrazolyl-pyridine) ligand from their respective $[M_3]$ subcomponents could also be traced by ^{1}H NMR, ES-MS, and single crystal X-ray diffraction.[21] We investigate here the reactivity with Cu(II) of a bis(2-hydroxyphenylpyrazolyl)-pyridine ligand (H_4L; Scheme 1) under strong basic conditions. H_4L exhibits several successive coordination pockets that should favor the assembly of certain

Received: June 25, 2013
Published: March 7, 2014

   dx.doi.org/10.1021/ic402647t | *Inorg. Chem.* 2014, 53, 3290−3297

Scheme 1. Representation of the Ligand H_4L

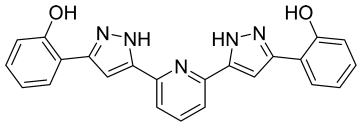

metal sequences within clusters.[22] However, its structure shows some flexibility, which allows for the observation of a variety of cluster topologies, compatible with maintaining certain structural motifs.[23,24] We show now that, when fully deprotonated, H_4L has a tendency to form a remarkable cyclic $[Cu_{16}L_8]$ cluster that can be reproducibly isolated and fully characterized. Interestingly, small variations in reaction conditions have allowed the crystallographic characterization of its building blocks, as well as one closely related product, $[Cu_{11}L_5(OH)_2(py)_{12}]$. The latter could be considered one more component in the complex equilibria that certainly coexist in solution before specific molecules separate as single crystals from these reaction systems.

RESULTS AND DISCUSSION

Synthesis. The structure of H_4L suggests that it may be a good ligand to study processes of self-assembly of coordination clusters, since it displays an array of donor atoms and coordination pockets, capable of binding several metals in adjacent positions. The disposition of these donor atoms, however, prevents the formation of molecular chains of metals arranged in a straight line. Instead, as seen in this Article, the combination of H_4L under strong basic conditions with Cu(II) ions leads to curved linear clusters that evolve as L^{4-} groups surrounding successions of metals which, forced by structural constraints, always describe a helical trajectory. Thus, the reaction of H_4L with $CuCl_2$ and NBu_4OH in pyridine/Et_2O produces crystals of the homoleptic cluster $(NBu_4)_2[Cu_7L_4]$ (**1**) after a process that could be described by the balanced eq 1.

$$7CuCl_2\cdot 2H_2O + 4H_4L + 16NBu_4OH \rightarrow \rightarrow (NBu_4)_2[Cu_7L_4] + 14NBu_4Cl + 30H_2O \quad (1)$$

The reproducibility of this reaction was established by multiple unit cell determinations from the crystalline product, as well as microanalysis experiments and ESI-MS determinations (Supporting Information Figure S1), which are consistent with the formulation.

The same reaction, using NaH as a base and hexane as precipitating solvent, allows the separation of different products. In fact, crystals of two different clusters may be obtained: the linear cluster $[Cu_{11}L_5(OH)_2(py)_{12}]$ (**2a**) and the cyclic aggregate $[Cu_{16}L_8(py)_6(H_2O)_3]$ (**2b**), which cannot be separated in the bulk, but only as single crystals by hand. These results show that the absence of a suitable cation changes the reaction and/or crystallization pathway toward the isolation of drastically different aggregates. The fact that the latter process yields two different products underscores that this reaction system leads to more than one accessible thermodynamic minimum. It was not possible to establish the exact variables to isolate reproducibly one or the other compound. Multiple single crystal X-ray diffraction determinations proved that only these two species crystallized. Interestingly, if the process is repeated while replacing the second solvent hexane by MeOH, it is possible to reproducibly obtain crystals of only a $[Cu_{16}]$ cluster almost identical to **2b**. The formula of this new product is $[Cu_{16}L_8(py)_6(MeOH)_2(H_2O)_2]$ (**3**), and its formation may be described by a balanced chemical eq 2.

Table 1. Crystal Data and Refinement for Compounds 1, 2a, 2b, and 3

	1	2a	2b	3
T [K]	100	100	100	100
empirical formula	$C_{134}H_{134}Cu_7N_{24}O_8$	$C_{180}H_{132}Cu_{11}N_{38}O_{12}$	$C_{239}H_{165}Cu_{16}N_{51}O_{19}$	$C_{245.5}H_{183.5}Cu_{16}N_{51.5}O_{23}$
fw [g/mol]	2653.42	3718.17	5071.85	5239.57
wavelength [Å]	0.7107	0.7749	0.7749	0.7107
cryst syst	orthorhombic	triclinic	triclinic	monoclinic
space group	$P2_12_12$	$P\bar{1}$	$P\bar{1}$	$C2/c$
a [Å]	18.4017(8)	16.809(14)	21.968(8)	40.052(6)
b [Å]	32.334(2)	18.756(16)	22.557(8)	41.569(6)
c [Å]	11.8948(5)	31.64(3)	25.407(9)	40.712(6)
α [deg]	90	92.148(13)	65.291(5)	90
β [deg]	90	98.901(12)	64.961(5)	117.881(4)
γ [deg]	90	94.909(11)	76.157(5)	90
V [Å^3]	7077.4(6)	9807(15)	10 333(6)	59 914(15)
Z	2	2	2	8
ρ [g/cm^3]	1.245	1.259	1.630	1.162
reflns	5583	16627	16264	20047
params	402	1192	1296	1670
restraints	118	127	32	24
R_{int}	0.0800	0.1382	0.0891	0.1729
R1 [$I > 2\sigma(I)$][a]	0.0946	0.1400	0.2020	0.0667
wR2 [all data][b]	0.2823	0.3811	0.4771	0.1697
GOF	1.077	1.139	1.106	0.896

[a] $R1 = \Sigma||F_o| - |F_c||/\Sigma|F_o|$. [b] $wR2 = (\Sigma[w(F_o^2 - F_c^2)^2]/\Sigma[w(F_o^2)^2])^{1/2}$.

dx.doi.org/10.1021/ic402647t | Inorg. Chem. 2014, 53, 3290−3297

$$16CuCl_2\cdot 2H_2O + 8H_4L + 32NaH + 6py + 2MeOH \rightarrow$$
$$\rightarrow [Cu_{16}L_8(py)_6(MeOH)_2(H_2O)_2] + 32NaCl + 32H_2$$
$$+ 30H_2O \quad (2)$$

The identity of **3** in the bulk was established as for compound **1** (several single crystal X-ray unit cell determinations and elemental analysis) except for the MS experiments, due to its nil solubility.

The fact that the precipitating solvent drives the isolation of only one product instead of two confirms the solubility (and thus, everything having to do with packing forces) as a determining factor in the nature of the solid that can be finally separated and studied.

Description of Structures. Crystallographic data for compounds **1**, **2a**, **2b**, and **3** are compiled in Table 1. Selected interatomic distances and angles are in Supporting Information Tables S1−S4. Although pertaining to different crystal systems and space groups, the structures of **2b** and **3** are built on very similar $[Cu_{16}]$ moieties. Only the latter is described here in detail, given the fact that one may prepare it, reproducibly, as a pure product. Structural details of **2b** can be found in the Supporting Information.

$(NBu_4)_2[Cu_7L_4]$ (1). The complex salt **1** crystallizes in the chiral orthorhombic space group $P2_12_12$. It is composed of a $[Cu_7L_4]^{2-}$ anion and two NBu_4^+ cations. The asymmetric unit is formed by one-half the content of the empirical formula, whereas the unit cell contains twice this formula. The anionic complex (Figure 1) is chiral; therefore, it is assumed that its

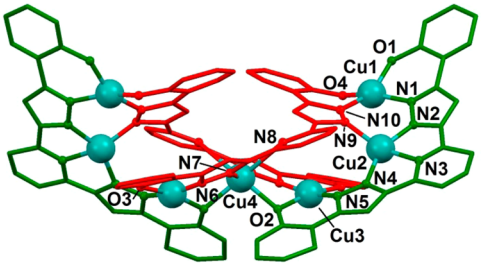

Figure 1. Representation of the anion of **1**, $[Cu_7L_4]^{2-}$, with unique heteroatoms labeled. Hydrogen atoms are not shown for clarity. Equivalent ligands are shown with the same color (red is in form B from Scheme 2 and green in form A).

enantiomer forms with identical probability and crystallizes within crystals with the opposite absolute chirality. The seven Cu(II) ions of the cluster are linked and chelated by four fully deprotonated H_4L ligands, coiled around the metals in an irregular helical sequence (Figure 2) by use of their phenolate, pyrazolate, and pyridine donor groups. The oxidation state of the metals is assigned on the basis of the magnetic response (see below) and charge balance considerations. The eventual presence of Cu(I) would require some of the phenol groups of the ligands to be protonated, something extremely unlikely under the strong basic conditions used for this reaction. A full bond valence sum (BVS) analysis supporting this assignment has been performed and can be found at the Supporting Information. The ligands of the cluster exhibit two different μ_4 coordination modes and conformations (A and B in Scheme 2). The molecule H_4L features five aromatic rings that, when combined with the formation of chelating rings with metals, favor planar arrangements. However, the fact that the rings are

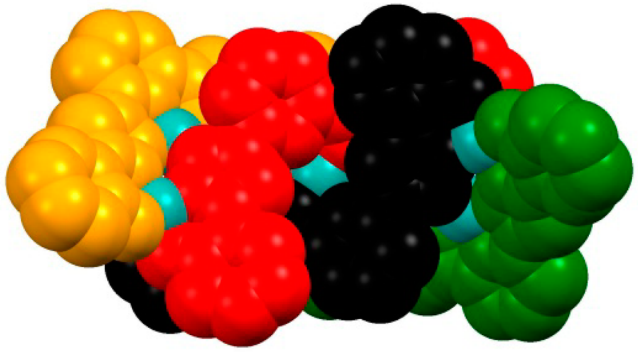

Figure 2. Space-filling representation of the anion of **1**, $[Cu_7L_4]^{2-}$, emphasizing its helical character. Hydrogen atoms are not shown for clarity.

Scheme 2. Coordination Modes of the Ligand L^{4-} Observed in Compounds 1, 2a, and 3, Emphasizing Two Observed Conformations: *syn,syn* (A, C) and *syn,anti* (B, D, E)

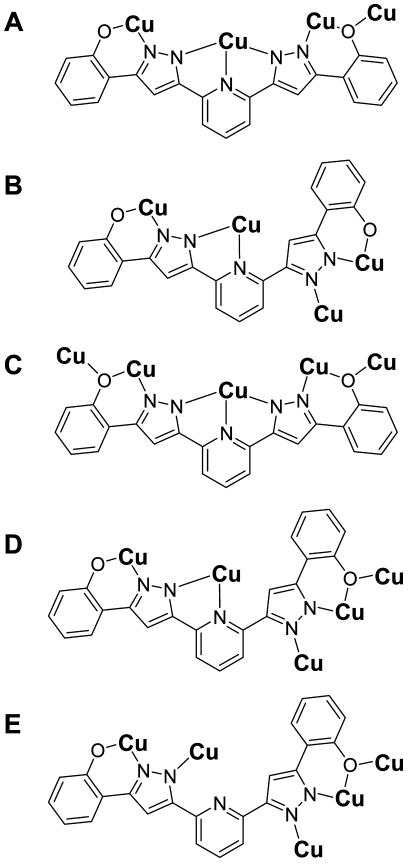

linked through C−C single bonds confers certain conformation flexibility upon the ligand. We have identified two conformations depending on the orientation of the hydroxyphenylpyrazolyl moieties with respect to the N atom of the central pyridyl ring: *syn,syn* and *syn,anti* (Scheme 2). This flexibility allows the concatenation of ligands of varying conformation around the metals, leading to linear sequences of ions as seen in **1** and the other compounds (see below).

The coordination geometry of the central metal atom (Cu4) is a rare and very distorted octahedral one of the type N_4O_2, with two very long Cu−N interactions in *cis* (2.724 Å), two intermediate Cu−O *cis* bonds (2.081 Å), and two short *trans*

dx.doi.org/10.1021/ic402647t | Inorg. Chem. 2014, 53, 3290−3297

contacts (1.87 Å), in what could be an irregular form of Jahn–Teller compression. The rest of the Cu(II) ions are intermediate between square planar and tetrahedral, with N_2O_2 (Cu1 and Cu3) and N_4 (Cu2) environments. Continuous shape measures (CShMs)[25] were used to establish the distance of each center to the ideal tetrahedron (Td) and square (Sq), respectively, revealing that in all cases the geometry is much closer to the latter. These distances are, in the Td/Sq format, 16.005/4.732, 20.515/3.932, and 23.804/1.200, for Cu1, Cu2, and Cu3, respectively. The distances between adjacent Cu(II) centers are 3.724(6) Å (Cu1···Cu2), 3.650(6) Å (Cu2···Cu3), and 3.231(6) Å (Cu3···Cu4). The crystal packing of the components of **1** occurs through van der Waals interactions, as analyzed by means of Hirshfeld surfaces[26,27] (see Supporting Information Figures S2–S4). This analysis reveals that the $[Cu_7]^{2-}$ clusters interact with each other through H···H interactions, forming layers that, in turn, are separated by arrays of NBu_4^+ cations (Supporting Information Figure S5). The latter establishes relatively strong C–H···π interactions with the aromatic rings of the Cu complex, in addition to H···H contacts (Supporting Information Figures S2–S4).

$[Cu_{11}L_5(OH)_2(py)_{12}]$ (2a). The unit cell of this compound is triclinic, from the $P\bar{1}$ space group, and contains two symmetry equivalent and enantiomeric $[Cu_{11}]$ clusters (Supporting Information Figure S6) together with two lattice molecules of pyridine. The cluster (Figure 3 and Supporting Information Figure S7) consists of a linear array of Cu(II) ions describing an irregular helical trajectory (Figure 4). BVS analysis (Supporting Information) supports the oxidation state assignments, which are consistent with the charge valence of the system and the fact that the product was generated under strong basic conditions. Again, the structure originates essentially from the succession of L^{4-} donors in the *syn,syn* and the *syn,anti* conformation.

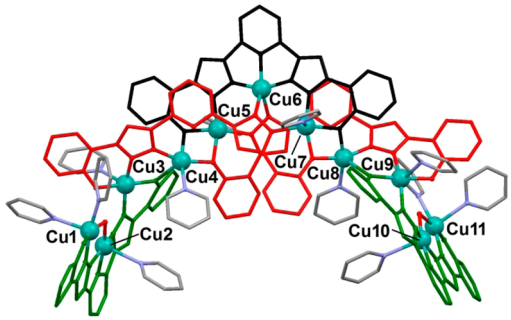

Figure 3. Representation of the complex $[Cu_{11}L_5(OH)_2(py)_{12}]$ (**2a**) with metal atoms labeled. Hydrogen atoms are not shown for clarity. Equivalent L^{4-} ligands are shown with the same color (black is in form C from Scheme 2, red in form E, and green in form A). For the rest of the atoms: gray, C; purple, N; red, O.

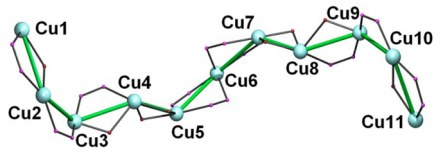

Figure 4. Representation of the metallic core of $[Cu_{11}L_5(OH)_2(py)_{12}]$ (**2a**). Contiguous Cu(II) ions are linked by a thick bar, as a guide to emphasize the irregular helical arrangement of these throughout the structure. The distances between these metal pairs are (in Å): 3.450(4) (Cu1···Cu2), 4.033(6) (Cu2···Cu3), 3.538(5) (Cu3···Cu4), 2.996(4) (Cu4···Cu5), 3.764(5) (Cu5···Cu6), 3.785(5) (Cu6···Cu7), 3.026(4) (Cu7···Cu8), 3.548(5) (Cu8···Cu9), 4.043(6) (Cu9···Cu10), and 3.518(6) (Cu10···Cu11).

In this complex we find five L^{4-} ligands in three different coordination modes: two μ_5 types (forms C and D of Scheme 2) and one μ_4 (form A). A major difference with respect to the structure of **1** is the presence in **2a** of one [Cu(II)–(μ–OH)–Cu(II)] bridge at each end of the molecule, which conditions the way in which the rest of the L^{4-} ligands organize around the metals ions and thus the final structure. The resulting arrangement also facilitates the binding of solvent pyridine molecules on the vacant coordination sites of the metals, conducive to the absence of four-coordinated centers. The only Cu(II) ion lacking solvent ligands is the central one (Cu6), which exhibits very distorted square pyramidal N_5 coordination environment (τ = 0.27).[28] Cu5, Cu7, Cu9, and Cu3 exhibit a geometry also closer to square pyramidal (τ = 0.18, 0.17, 0.29, and 0.22, respectively) with equatorial N_2O_2 environments (*cis* for Cu5, Cu7 and *trans* for Cu9, Cu3) provided by two L^{4-} ligands, and axial positions occupied by pyridine. The N_2O_3 donors around Cu4 and Cu8 impart coordination geometries also quite close to a square pyramid (τ = 0.12 and 0.10, respectively), while the surroundings of Cu1 and Cu11 (N_3O_2) and Cu2 and Cu10 (N_2O_3), involving bridging OH^- ligands, exhibit the same geometry (τ = 0.13, 0.09, 0.15, and 0.19, respectively). The distances between adjacent metal atoms within the string of complex **2a** are given at the legend of Figure 4 and Supporting Information Table S2.

The packing of molecules of **2** in the lattice occurs *via* weak interactions mainly involving the numerous aromatic rings crowding the periphery of the cluster. In particular, a strong complementary π···π interaction has been identified that serves to organize the complexes as dimers within the crystal (Supporting Information Figure S8).

$[Cu_{16}L_8(py)_6(MeOH)_2(H_2O)_2]$ (3). Complex **3** crystallizes in the monoclinic space group *C*2/*c*. The asymmetric unit contains one $[Cu_{16}]$ cluster, five and a half molecules of pyridine, two molecules of methanol, and one of water. The unit cell is remarkably large; it contains a total of eight asymmetric units. The coordination cluster is chiral, and enantiomers are present in equal amounts within the lattice. It consists of a ring of 16 Cu(II) ions (Figure 5, Figure S10 in the Supporting Information, and Figure 6) with the overall saddle shape, held together exclusively by eight L^{4-} ligands present in two different μ_5 coordination modes (C and D in Scheme 2) by use of bridging phenolate and pyrazolate groups and through their central pyridine moiety. Solvent molecules of pyridine (six), methanol (two), or water (two) complete the coordination around the metals. There are three types of chelate rings: N,N five-membered (Cu8 and Cu16), N,O six-membered (Cu1, Cu3, Cu5, Cu7, Cu9, Cu11, Cu13, and Cu15), and N,N,N (Cu2, Cu6, Cu10, and Cu14) of the bis-pyrazolylpyridine type. The only metals not partaking of any chelate rings are Cu4 and Cu12 (NO_5 environment, τ = 0.28 and 0.30). Atoms Cu1, Cu7, Cu9, and Cu15 are four-coordinate (N_2O_2, with distances to the square and the perfect tetrahedron, in the Td/Sq format, of 19.687/2.579, 22.361/1.728, 21.718/1.934, and 21.334/2.003, respectively). There are four metals with an N_4O environment, involving one water or one methanol solvent ligand each (Cu2, Cu6, Cu10, and Cu14, with τ values of 0.17, 0.14, 0.15, and 0.15, respectively), and

dx.doi.org/10.1021/ic402647t | Inorg. Chem. 2014, 53, 3290–3297

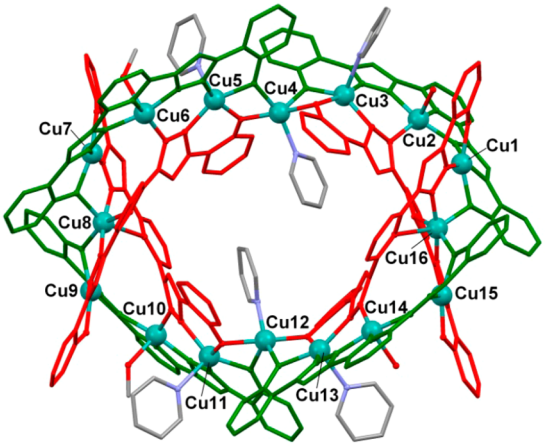

Figure 5. Representation of the complex $[Cu_{16}L_8(py)_6(MeOH)_2(H_2O)_2]$ (**3**) with metal atoms labeled. Hydrogen atoms are not shown for clarity. Equivalent L^{4-} ligands are shown with the same color (red is in form D from Scheme 2 and green in form C). For the rest of the atoms: gray, C; purple, N; red, O.

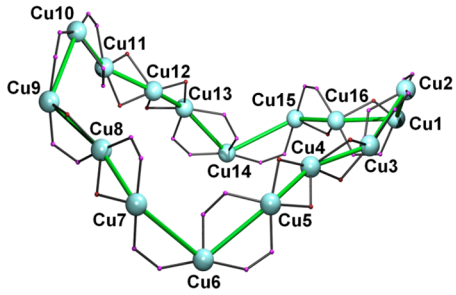

Figure 6. Representation of the metallic core of $[Cu_{16}L_8(py)_6(MeOH)_2(H_2O)_2]$ (**3**). The contiguous Cu(II) ions are linked by a thick bar, as a guide to emphasize the "horse seat" shape of the ring. The distances between these metal pairs are (in Å) as follows: 4.020(4) (Cu1···Cu2), 3.785(4) (Cu2···Cu3), 3.086(3) (Cu3···Cu4), 3.071(3) (Cu4···Cu5), 3.750(4) (Cu5···Cu6), 3.919(4) (Cu6···Cu7), 3.321(3) (Cu7···Cu8), 3.335(4) (Cu8···Cu9), 3.969(4) (Cu9···Cu10), 3.782(4) (Cu10···Cu11), 3.081(3) (Cu11···Cu12), 3.078(3) (Cu12···Cu13), 3.759(4) (Cu13···Cu14), 3.945(4) (Cu14···Cu15), 3.324(3) (Cu15···Cu16), 3.309(3) (Cu16···Cu1).

four metals with a N_3O_2 donor set (Cu3, Cu5, Cu11, and Cu13) that engage one axial pyridine each, exhibiting τ values of 0.34, 0.02, 0.27, and 0.09, respectively. Finally, Cu8 and Cu16 exhibit distorted octahedral N_2O_4 surroundings formed by donors furnished by three different L^{4-} ligands. The assignment of the oxidation state +2 of these metals is made under the same rationale as for complex **1** (see Supporting Information for BVS analysis). The legend of Figure 6 features the list of adjacent Cu···Cu distances. As an estimation of the width of this metalloring, the longest encountered intramolecular Cu···Cu vector measures 18.158(4) Å.

Structural Correlations. A detailed comparison of the molecular structures of compounds **1**, **2a**, **2b**, and **3** reveals that they follow a hierarchical relationship of increasing complexity. Thus, it is worth noticing (Figure 7) that almost the totality of the complex anion $[Cu_7L_4]^{2-}$ of **1** is contained within the cluster $[Cu_{11}L_5(OH)_2(py)_{12}]$ (**2a**). In fact, it is clear when comparing both structures that an important difference between both is the presence of two μ-OH^- ligands in **2a**, which necessarily exerts an impact on the way that the L^{4-}

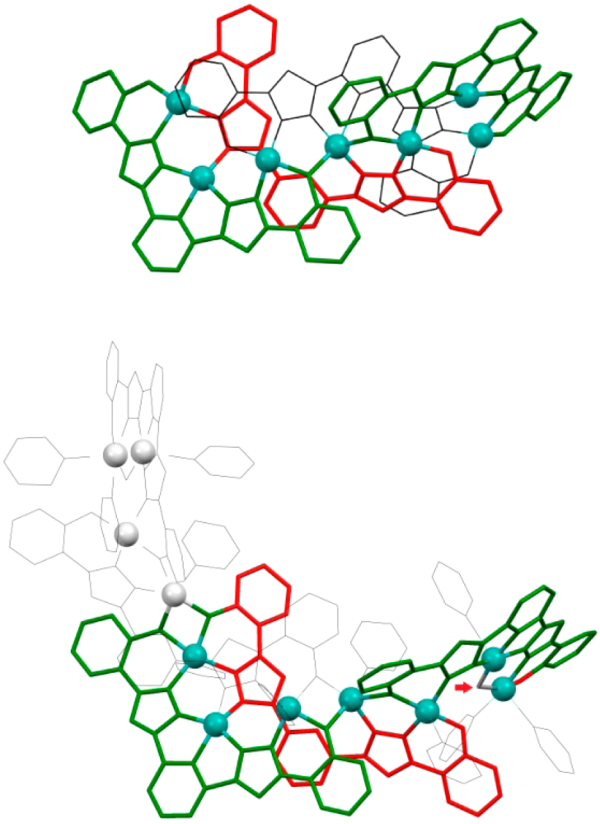

Figure 7. Representation of the anion $[Cu_7L_4]^{2-}$ of **1** (top) emphasizing the portion that is also contained within the cluster $[Cu_{11}L_5(OH)_2(py)_{12}]$ (**2a**), as highlighted within the structure of the latter (bottom). The red arrow indicates the μ-OH^-, absent in the $[Cu_7]$ cluster.

ligands develop the molecular chain around the metals. In a more remarkable way, a careful inspection of the cluster $[Cu_{16}L_8(py)_6(H_2O)_3]$ (**2b**) or $[Cu_{16}L_8(py)_6(MeOH)_2(H_2O)_2]$ (**3**) shows that the $[Cu_{16}]$ ring is in fact formed through the bridging of two $[Cu_7L_4]^{2-}$ units (seen in **1** to exist as independent species, also in solution, as demonstrated by MS measurements; Supporting Information Figure S1) by means of two additional Cu(II) cations (Figure 8). In this assembly, the $[Cu_7L_4]^{2-}$ anions can be seen as performing a role of cluster ligands, chelating two copper metals by means of the oxygen atoms from their external phenolate moieties. It is indeed very likely that the formation of $[Cu_7L_4]^{2-}$ units precedes the formation of the $[Cu_{16}]$ rings **2b** and **3**, before the cycles are closed with help of additional Cu(II) ions. However, this sequential succession of events cannot be asserted with certainty without additional evidence. The fact that very subtle changes in reaction parameters (the combination of solvents and/or the nature of the base) allows crystallization of three different structural types indicates that these molecular arrangements constitute shallow minima in the potential surface, where solubility and packing parameters must play a crucial role in determining the product finally observed as single crystal. It is quite apparent for example that the presence of NBu_4^+ cations constitutes a strong driving force toward the crystallization of the salt $(NBu_4)_2[Cu_7L_4]$ (**1**). On the other hand, the structural analysis of the $[Cu_{16}]$ complexes suggests the possibility of utilizing the complex salt $(NBu_4)_2[Cu_7L_4]$ (**1**)

dx.doi.org/10.1021/ic402647t | Inorg. Chem. 2014, 53, 3290−3297

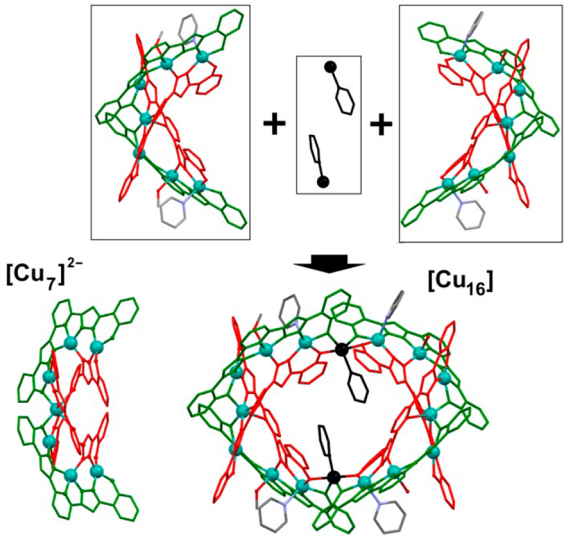

Figure 8. Representation of the mechanism of formation of $[Cu_{16}L_8(py)_6(MeOH)_2(H_2O)_2]$ (**3**) as the linking of two anionic $[Cu_7L_4]^{2-}$ cluster ligands *via* coordination to two Cu(II) ions. At the bottom are represented the true structures of **3** and of the anion of **1**.

as starting material in coordination chemistry reactions for the designed preparation of $[Cu_{14}M_2]$ heterometallic rings.

Bulk Magnetization Properties. The bulk magnetization of complexes $(NBu_4)_2[Cu_7L_4]$ (**1**) and $[Cu_{16}L_8(py)_6(MeOH)_2(H_2O)_2]$ (**3**) was examined under a constant magnetic field of 1 T in the 2−300 K temperature range. The results are shown in Figure 9, in the form of $\chi_M T$

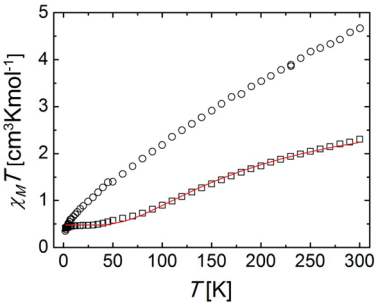

Figure 9. $\chi_M T$ vs T plots of $(NBu_4)_2[Cu_7L_4]$ (**1**) and $[Cu_{16}L_8(py)_6(MeOH)_2(H_2O)_2]$ (**3**). The solid line is a fit of the experimental data, by fixing the J values to these obtained from DFT calculations (see text).

versus T plots, where χ_M is the molar paramagnetic susceptibility. The values of $\chi_M T$ at 300 K are 2.30 and 4.58 cm^3 K mol^{-1} for **1** and **3**, respectively, well below the numbers expected for 7 and 16 isolated Cu(II) ions, respectively, with g = 2, which would be 2.62 and 6.00 cm^3 K mol^{-1}. This suggests the presence of antiferromagnetic interactions within both molecules, leading to spin ground states of $S = {}^1/_2$ (**1**) and S = 0 (**3**), respectively. The size of $(NBu_4)_2[Cu_7L_4]$ (**1**) renders it amenable to fitting the magnetic data by matrix diagonalization using reasonable computer resources. The energy of the magnetic exchange within the cluster may be described by the Heisenberg spin Hamiltonian of eq 3.

$$H = -2J_1(S_1S_2 + S_{1\#}S_{2\#}) - 2J_2(S_2S_3 + S_{2\#}S_{3\#}) - 2J_3(S_3S_4 + S_{3\#}S_4) \quad (3)$$

In the above equation, the labels of the atomic spin moments correspond to these from Figure 1. The experimental data could be fit perfectly using the program CLUMAG.[29] However, since both J_1 and J_3 were found to be strongly antiferromagnetic, the value of J_2 did not have an influence on the overall shape of the curve, and the procedure had a tendency to attribute to it unrealistically high ferromagnetic values. It was found thus more reasonable to obtain estimates of these interactions by means of DFT calculations.

The DFT J values were obtained after calculating the electronic energy of different spin configurations and solving a set of linear equations. Of these values, the parameter that was undetermined from the original fitting was then inserted as a fixed term in a novel matrix diagonalization fitting, which then led to a best set of parameters that reproduced well the experimental data (Figure 9): J_1 = −112.0 cm^{-1}, J_2 = −36.0 cm^{-1}, and J_3 = −90.0 cm^{-1}, and a g = 2.26. These values may be discussed in light of the parameters reported in the literature for the corresponding exchange pathways. Thus, the value of J_1, corresponding to a double −NN− pyrazolato bridge, is near the weaker end of the range usually observed within this motif, hitherto found approximately within the limits −70 and −300 cm^{-1}.[30−35] In this type of pathway, the higher the coplanarity of the [Cu−(μ-pz)$_2$−Cu] moiety, the more efficient the exchange. Thus, an increase of the Cu−N−N−Cu torsion, of the dihedral angle between pyrazolato rings, or of the distortion from tetragonal coordination symmetry diminishes the magnitude of −J. In this case, Cu1 is considerably distorted from the square plane (see CShMs above), whereas the torsion angles are significant: 18.29° and 39.52°. The bridge through *only* one pyrazolato group (here described by J_2) is susceptible of experiencing higher distortions, thus detrimental to an efficient exchange. This and the fact of dividing by two the number of pathways for the calculations[36] explains that much weaker values have been obtained with this method. In complex **1**, Cu2 and Cu3 exhibit significant distortions from a perfect square plane, the magnetic orbitals ($d_{x^2-y^2}$) are far from being coplanar, and the Cu−N−N−Cu torsion angle is 28.85°. J_2 is within the range observed in the majority of compounds[36−39] (−12.34 to −155 cm^{-1}; the latter limit was proposed only as a limiting threshold,[37] thus, the range could be narrower). Finally, J_3 represents the coupling between a distorted octahedral Cu(II) ion and an approximately square planar one, mediated by both a pyrazolato and a phenoxide bridge. Given the rare distortion (Jahn−Teller compression) featured by the octahedral Cu(II) ion (Cu4), it is not clear what its magnetic orbital is. Likely, it is quite similar to a d_{z^2} orbital; thus, it interacts with the magnetic orbital of Cu3 ($d_{x^2-y^2}$) *via* the pyrazolato bridge. The interaction through the phenoxide group is therefore less efficient. These two bridges are known to facilitate antiferromagnetic couplings between Cu(II) ions.[40−42] The very rare geometry of the bridging moiety encountered here, however, precludes any meaningful comparison. The interpretations from these calculations and measurements are consistent with the results obtained from variable temperature, X-band EPR measurements. Powder EPR spectra were obtained at various temperatures from 4 to 302 K (Supporting Information Figure S11). As expected from a paramagnetic $S = {}^1/_2$ ground state resulting from antiferromagnetic interactions, a broad isotropic

dx.doi.org/10.1021/ic402647t | Inorg. Chem. 2014, 53, 3290−3297

signal centered at g = 2.11 is observed at room temperature, which becomes gradually more intense, sharper, and more axial as the temperature decreases, until a strong signal with $g_\perp$ = 2.04 is observed at 4 K, while a parallel component that seems to exhibit hyperfine splitting from coupling with the Cu nucleus is appreciable. No half field resonances were observed.

The lack of solubility precludes solution studies of compounds **2a**, **2b**, and **3** once they form, something that would be of great value to understand the processes of self-assembly unveiled here.

CONCLUSIONS

The ligand H_4L under strong basic conditions reacts with Cu(II) in pyridine to produce a cyclic $[Cu_{16}L_8]$ molecular cluster. The formation of this aggregate seems to occur through the assembly of two $[Cu_7L_8]^{2-}$ subunits acting as *cluster-ligands*, via two bridging additional Cu(II) ions. Evidence of this is that the heptanuclear subunit can be obtained independently in the presence of an appropriate counterion (such as NBu_4^+). Also, the process of formation of the $[Cu_{16}L_8]$ cycle is certainly accompanied by the coexistence of other products. One such compound could be characterized crystallographically and identified as the cluster $[Cu_{11}L_5(OH)_2(py)_{12}]$, which, on the other hand, could not be isolated. It features two [Cu−(OH)−Cu] bridges between adjacent Cu ions fixed by L^{4-}. Understanding this mechanism of formation of the $[Cu_{16}]$ cycles could allow the deliberate preparation of other complex aggregates such as heterometallic $[Cu_{14}M_2L_8]$ rings.

EXPERIMENTAL SECTION

Synthesis. The ligand 2,6-bis(5-(2-hydroxyphenyl)-pyrazol-3-yl)-pyridine) (H_4L) was prepared according to a procedure published by us.[43] Solvents and reagents were used as received without purification.

$(NBu_4)_2[Cu_7L_4]$ (1). A light yellow solution of H_4L (50.6 mg, 0.13 mmol) and NBu_4OH (0.51 mL, 0.51 mmol) in pyridine (15 mL) was added dropwise to a blue solution of $CuCl_2{\cdot}2H_2O$ (48.0 mg, 0.28 mmol) in pyridine (15 mL). The mixture was stirred under reflux for 2 h and then cooled down to room temperature. A very small amount of a dark solid was removed by filtration, and the dark green filtrate was layered with Et_2O. Dark green crystals formed in 24 h, in 25% yield. Anal. Calcd (Found) for **1**(+5.6H_2O): C 57.37 (57.15), H 5.25 (5.02), N 11.87 (11.90). IR (KBr pellet, cm^{-1}): 3441 sb, 2960 w, 2870 w, 1639 w, 1597 m, 1559 w, 1501 w, 1471 s, 1301 s, 1273 m, 1248 w, 1147 w, 1131 w, 1035 w, 849 w, 785 m, 748 m, 664 w, 587 w. ESI MS: m/z = 1004.4732 $[Cu_7(L)_4]^{2-}$ (z = 2).

$[Cu_{11}L_5(OH)_2(py)_{12}]$ (2a) + $[Cu_{16}L_8(py)_6(H_2O)_3]$ (2b). A suspension of H_4L (50.6 mg, 0.13 mmol) and 60% NaH (27.6 mg, 0.51 mmol) in pyridine (15 mL) was added dropwise to a blue solution of $CuCl_2{\cdot}2H_2O$ (48.0 mg, 0.28 mmol) in pyridine (15 mL). The mixture was stirred under reflux for 2 h and then cooled down to room temperature. A very small amount of a dark solid was removed by filtration, and the dark green filtrate was layered with hexane. Dark green crystals of **2a** and **2b** were obtained after 15 days.

$[Cu_{16}L_8(py)_6(MeOH)_2(H_2O)_2]$ (3). A suspension of H_4L (50.6 mg, 0.13 mmol) and 60% NaH (27.6 mg, 0.51 mmol) in pyridine (15 mL) was added dropwise to a blue solution of $CuCl_2{\cdot}2H_2O$ (48.0 mg, 0.28 mmol) in pyridine (15 mL). The mixture was stirred under reflux for 2 h and then cooled down to room temperature. A very small amount of a dark solid was removed by filtration, and the dark green filtrate was layered with MeOH. Dark green crystals were obtained after six days in 5% yield. Anal. Calcd (Found) for **3**(−2MeOH + 7H_2O): C 53.71 (53.37), H 3.20 (2.86), N 13.46 (13.38). IR (KBr pellet, cm^{-1}): 3443 sb, 1630 m, 1599 m, 1568 m, 1503 w, 1470 s, 1300 m, 1268 m, 1241 w, 1146 w, 1126 w, 1070 w, 1036 w, 847 w, 786 w, 749 m, 701 w, 666 w, 588 w.

X-ray Crystallography. Data for compounds **1** and **3** were collected at 100 K, respectively, on a dark green block and plate using Mo Kα radiation (λ = 0.7107 Å) on a Bruker APEX II QUAZAR diffractometer equipped with a microfocus multilayer monochromator. Data for compounds **2a** and **2b** were obtained at 100 K, respectively, on a green block and a dark green plate with a Bruker APEX II CCD diffractometer on the Advanced Light Source beamline 11.3.1 at Lawrence Berkeley National Laboratory, from a silicon 111 monochromator (λ = 0.7749 Å). Data reduction and absorption corrections were performed with SAINT and SADABS, respectively.[44] The structures were solved and refined on F^2 using the SHELX-TL suite.[45] Repeatedly for all four compounds and on several crystals, there was significant diffraction only up to ca. 1.04−1.1 Å resolution. The present data were thus cut at the relevant resolution for which $I/\sigma(I)$ was below 2, and completeness dropped abruptly. This results in all four cases in low values of θ_{max}, θ_{full} and poor data over parameter ratios. This is likely related to poor crystallinity due to loss of diffuse lattice solvent. Because there were too few observed reflections with respect to the number of parameters required to refine all non-hydrogens anisotropically, all carbon atoms of the main residues and all lattice molecules were refined isotropically. In the case of compound **2b**, only the copper atoms were refined anisotropically. In all four structures, large void space remained at the end of the refinement with only diffuse electron density. The SQUEEZE routine as implemented within PLATON[46,47] was used to analyze and take into account these voids and the corresponding lattice solvent content, resulting in significant improvement of the agreement indices. The structure of **2b** could initially only be solved in $P1$, with two slightly different $[Cu_{16}]$ moieties, but then refined satisfactorily in the centrosymmetric $P\bar{1}$ with only one $[Cu_{16}]$. The poor quality of this structure, which however unambiguously proves the identity of the compound, is thus likely related to some disorder of the whole $[Cu_{16}]$. Crystallographic and refinement parameters are summarized in Table 1. Selected bond distances and angles are given in Supporting Information Tables S1−S4.

Physical Measurements. Variable-temperature magnetic susceptibility data were obtained with a Quantum Design MPMS5 SQUID magnetometer. Pascal's constants were used to estimate diamagnetic corrections to the molar paramagnetic susceptibility. The elemental analysis was performed with a Elemental Microanalyzer (A5), model Flash 1112, at the Servei de Microanàlisi of CSIC, Barcelona, Spain. IR spectra were recorded as KBr pellet samples on a Nicolet AVATAR 330 FTIR spectrometer. X-Band (9.42 GHz) EPR spectra were determined with powdered samples on a Bruker ESP300E spectrometer, with a liquid helium cryostat. Negative ion ESI TOF mass spectrometry experiments were performed on an LC/MSD-TOF (Agilent Technologies) at the Unitat d'Espectrometria de Masses de Caracterització Molecular (CCiT) of the Universitat de Barcelona. The experimental parameters were as follows: capillary voltage 4 kV, gas temperature 325 °C, nebulizing gas pressure 15 psi, drying gas flow 7.0 L min^{-1}, and fragmentor voltage ranging from 175 to 300 V. Samples (μL) were introduced into the source by a HPLC system (Agilent 1100), using a mixture of DMSO/MeOH (1/100) as eluent (200 μL min^{-1}).

DFT Calculations. The DFT J values have been obtained after calculating the electronic energy of different spin configurations and solving a set of linear equations, as previously described.[48] These energy calculations have been carried out with the GAUSSIAN 09 package[49] using the B3LYP exchange-correlation functional,[50] an Ahlrichs TZV basis set[51] for the Cu(II) ions, and a 6-31G basis set[52] for the rest of the atoms.

ASSOCIATED CONTENT

Supporting Information

Hirshfeld surface analysis, additional crystallographic figures and information, EPR spectra, and ESI-MS spectrographs. Crystallographic data in CIF format. This material is available free of charge via the Internet at http://pubs.acs.org. All crystallographic details also can be found with CCDC numbers

dx.doi.org/10.1021/ic402647t | Inorg. Chem. 2014, 53, 3290−3297

928758 (**1**), 928759 (**2a**), 935796 (**2b**), and 928760 (**3**). These data can be obtained free of charge from The Cambridge Crystallographic Data Centre via www.ccdc.cam.ac.uk/data_request/cif.

AUTHOR INFORMATION

Corresponding Author

*E-mail: guillem.aromi@qi.ub.es.

Notes

The authors declare no competing financial interest.

ACKNOWLEDGMENTS

G.A. thanks the Generalitat de Catalunya for the prize *ICREA Academia 2008*, for excellence in research, and the ERC for a Starting Grant (258060 FuncMolQIP). The authors thank former Spanish MICINN for funding through CTQ2009-06959 (G.A., G.A.C., D.A.), current Spanish MINECO for funding through MAT2011-24284 (O.R.), CTQ2012-32247 (G.A.), a "Ramón y Cajal" Fellowship (J.R.-A.), and a Ph.D. grant to S.V. The Advanced Light Source (S.J.T.) is supported by the Director, Office of Science, Office of Basic Energy Sciences of the U.S. Department of Energy under Contract DE-AC02-05CH11231.

REFERENCES

(1) Aromí, G.; Aubin, S. M. J.; Bolcar, M. A.; Christou, G.; Eppley, H. J.; Folting, K.; Hendrickson, D. N.; Huffman, J. C.; Squire, R. C.; Tsai, H. L.; Wang, S.; Wemple, M. W. *Polyhedron* **1998**, *17*, 3005−3020.

(2) Winpenny, R. E. P. *J. Chem. Soc., Dalton Trans.* **2002**, 1−10.

(3) Milios, C. J.; Stamatatos, T. C.; Perlepes, S. P. *Polyhedron* **2006**, *25*, 134−194.

(4) Bagai, R.; Christou, G. *Chem. Soc. Rev.* **2009**, *38*, 1011−1026.

(5) Aromí, G.; Bhaduri, S.; Artus, P.; Folting, K.; Christou, G. *Inorg. Chem.* **2002**, *41*, 805−817.

(6) Papaefstathiou, G. S.; Perlepes, S. P.; Escuer, A.; Vicente, R.; Font-Bardia, M.; Solans, X. *Angew. Chem., Int. Ed.* **2001**, *40*, 884−886.

(7) Sessoli, R.; Tsai, H. L.; Schake, A. R.; Wang, S. Y.; Vincent, J. B.; Folting, K.; Gatteschi, D.; Christou, G.; Hendrickson, D. N. *J. Am. Chem. Soc.* **1993**, *115*, 1804−1816.

(8) Zhang, P.; Guo, Y.-N.; Tang, J. *Coord. Chem. Rev.* **2013**, *257*, 1728−1763.

(9) Aromí, G.; Brechin, E. K. *Struct. Bonding (Berlin)* **2006**, *122*, 1−67.

(10) Nayak, S.; Evangelisti, M.; Powell, A. K.; Reedijk, J. *Chem.—Eur. J.* **2010**, *16*, 12865−12872.

(11) Evangelisti, M.; Brechin, E. K. *Dalton Trans.* **2010**, *39*, 4672−4676.

(12) Timco, G. A.; Faust, T. B.; Tuna, F.; Winpenny, R. E. P. *Chem. Soc. Rev.* **2011**, *40*, 3067−3075.

(13) Aromí, G.; Aguilà, D.; Gamez, P.; Luis, F.; Roubeau, O. *Chem. Soc. Rev.* **2012**, *41*, 537−546.

(14) Ward, M. D.; Raithby, P. R. *Chem. Soc. Rev.* **2013**, *42*, 1619−1636.

(15) Piguet, C.; Bernardinelli, G.; Hopfgartner, G. *Chem. Rev.* **1997**, *97*, 2005−2062.

(16) Dawe, L. N.; Shuvaev, K. V.; Thompson, L. K. *Chem. Soc. Rev.* **2009**, *38*, 2334−2359.

(17) Ismayilov, R. H.; Wang, W.-Z.; Lee, G.-H.; Yeh, C.-Y.; Hua, S.-A.; Song, Y.; Rohmer, M.-M.; Bénard, M.; Peng, S.-M. *Angew. Chem., Int. Ed.* **2011**, *50*, 2045−2048.

(18) Zhu, L. G.; Peng, S. M. *Chin. J. Inorg. Chem.* **2002**, *18*, 117−124.

(19) Saalfrank, R. W.; Maid, H.; Scheurer, A. *Angew. Chem., Int. Ed.* **2008**, *47*, 8794−8824.

(20) Newton, G. N.; Onuki, T.; Shiga, T.; Noguchi, M.; Matsumoto, T.; Mathieson, J. S.; Nihei, M.; Nakano, M.; Cronin, L.; Oshio, H. *Angew. Chem., Int. Ed.* **2011**, *50*, 4844−4848.

(21) Stephenson, A.; Sykes, D.; Ward, M. D. *Dalton Trans.* **2013**, *42*, 6756−6767.

(22) Craig, G. A.; Roubeau, O.; Ribas-Ariño, J.; Teat, S. J.; Aromí, G. *Polyhedron* **2013**, *52*, 1369−1374.

(23) Costa, J. S.; Barrios, L. A.; Craig, G. A.; Teat, S. J.; Luis, F.; Roubeau, O.; Evangelisti, M.; Camon, A.; Aromí, G. *Chem. Commun.* **2012**, *48*, 1413−1415.

(24) Costa, J. S.; Craig, G. A.; Barrios, L. A.; Roubeau, O.; Ruiz, E.; Gómez-Coca, S.; Teat, S. J.; Aromí, G. *Chem.—Eur. J.* **2011**, *17*, 4960−4963.

(25) Alvarez, S.; Alemany, P.; Casanova, D.; Cirera, J.; Llunell, M.; Avnir, D. *Coord. Chem. Rev.* **2005**, *249*, 1693−1708.

(26) McKinnon, J. J.; Mitchell, A. S.; Spackman, M. A. *Chem.—Eur. J.* **1998**, *4*, 2136−2141.

(27) Spackman, M. A.; Jayatilaka, D. *CrystEngComm* **2009**, *11*, 19−32.

(28) Addison, A. W.; Rao, T. N.; Reedijk, J.; van Rijn, J.; Verschoor, G. C. *J. Chem. Soc., Dalton Trans.* **1984**, 1349−1356.

(29) Gatteschi, D.; Pardi, L. *Gazz. Chim. Ital.* **1993**, *123*, 231.

(30) Noble, A.; Olguín, J.; Clérac, R.; Brooker, S. *Inorg. Chem.* **2010**, *49*, 4560−4569.

(31) Mokuolu, Q. F.; Foguet-Albiol, D.; Jones, L. F.; Wolowska, J.; Kowalczyk, R. M.; Kilner, C. A.; Christou, G.; McGowan, P. C.; Halcrow, M. A. *Dalton Trans.* **2007**, 1392−1399.

(32) Miranda, C.; Escartí, F.; Lamarque, L.; García-España, E.; Navarro, P.; Latorre, J.; Lloret, F.; Jiménez Hermás, R.; Yunta María, J. R. *Eur. J. Inorg. Chem.* **2005**, *2005*, 189−208.

(33) Hu, T.-L.; Li, J.-R.; Liu, C.-S.; Shi, X.-S.; Zhou, J.-N.; Bu, X.-H.; Ribas, J. *Inorg. Chem.* **2005**, *45*, 162−173.

(34) Drew, M. G. B.; Yates, P. C.; Esho, F. S.; Trocha-Grimshaw, J.; Lavery, A.; McKillop, K. P.; Nelson, S. M.; Nelson, J. *J. Chem. Soc., Dalton Trans.* **1988**, 2995−3003.

(35) Matsushima, H.; Hamada, H.; Watanabe, K.; Koikawa, M.; Tokii, T. *J. Chem. Soc., Dalton Trans.* **1999**, 971−978.

(36) Zhang, H.; Fu, D.; Ji, F.; Wang, G.; Yu, K.; Yao, T. *J. Chem. Soc., Dalton Trans.* **1996**, 3799−3803.

(37) Mann, K. L. V.; Psillakis, E.; Jeffery, J. C.; Rees, L. H.; Harden, N. M.; McCleverty, J. A.; Ward, M. D.; Gatteschi, D.; Totti, F.; Mabbs, F. E.; McInnes, E. J. L.; Riedi, P. C.; Smith, G. M. *J. Chem. Soc., Dalton Trans.* **1999**, 339−348.

(38) Iskander, M. F.; Khalil, T. E.; Haase, W.; Werner, R.; Svoboda, I.; Fuess, H. *Polyhedron* **2001**, *20*, 2787−2798.

(39) Driessen, W. L.; Chang, L.; Finazzo, C.; Gorter, S.; Rehorst, D.; Reedijk, J.; Lutz, M.; Spek, A. L. *Inorg. Chim. Acta* **2003**, *350*, 25−31.

(40) Bai, Y.-L.; Tangoulis, V.; Huang, R.-B.; Zheng, L.-S.; Tao, J. *Chem.—Eur. J.* **2009**, *15*, 2377−2383.

(41) Tong, J.-P.; Sun, X.-J.; Tao, J.; Huang, R.-B.; Zheng, L.-S. *Inorg. Chem.* **2010**, *49*, 1289−1291.

(42) Mikuriya, M.; Nakadera, K.; Lim, J.-W. *Synth. React. Inorg. Met.-Org. Chem.* **2002**, *32*, 117−125.

(43) Craig, G. A.; Barrios, L. A.; Costa, J. S.; Roubeau, O.; Ruiz, E.; Teat, S. J.; Wilson, C. C.; Thomas, L.; Aromí, G. *Dalton Trans.* **2010**, *39*, 4874−4881.

(44) *SAINT, SADABS and SHELXTL*; Bruker AXS Inc.: Madison, WI.

(45) Sheldrick, G. M. *Acta Crystallogr., Sect. A* **2008**, *64*, 112−122.

(46) *PLATON, A Multipurpose Crystallographic Tool*; Utrecht University: Utrecht, The Netherlands, 2008.

(47) Spek, A. *J. Appl. Crystallogr.* **2003**, *36*, 7−13.

(48) Ruiz, E.; Rodriguez-Fortea, A.; Cano, J.; Alvarez, S.; Alemany, P. *J. Comput. Chem.* **2003**, *24*, 982−989.

(49) *Gaussian 09, Revision A.1*; Gaussian, Inc.: Wallingford, CT, 2009.

(50) Becke, A. D. *J. Chem. Phys.* **1993**, *98*, 5648−5652.

(51) Schafer, A.; Huber, C.; Ahlrichs, R. *J. Chem. Phys.* **1994**, *100*, 5829−5835.

(52) Ditchfield, R.; Hehre, W. J.; Pople, J. A. *J. Chem. Phys.* **1971**, *54*, 724−728.